Ground state of superheavy elements with $120 \leqslant Z \leqslant 170$: Systematic study of the electron-correlation, Breit, and QED effects

I. M. Savelyev [1], M. Y. Kaygorodov [1], Y. S. Kozhedub [1], A. V. Malyshev [1], I. I. Tupitsyn [1], and V. M. Shabaev [1,2]

[1]*Department of Physics, St. Petersburg State University, 7/9 Universitetskaya nab., 199034 St. Petersburg, Russia*

[2]*National Research Centre "Kurchatov Institute" B.P. Konstantinov Petersburg Nuclear Physics Institute, Gatchina, Leningrad District 188300, Russia*

(Received 5 January 2023; accepted 28 February 2023; published 6 April 2023)

For superheavy elements with atomic numbers $120 \leqslant Z \leqslant 170$, the concept of the ground-state configuration is being reexamined. To this end, relativistic calculations of the electronic structure of the low-lying levels are carried out by means of the Dirac-Fock and configuration-interaction methods. The magnetic and retardation parts of the Breit interaction as well as the QED effects are taken into account. The influence of the relativistic, QED, and electron-electron correlation effects on the determination of the ground state is analyzed.

DOI: 10.1103/PhysRevA.107.042803

I. INTRODUCTION

Mendeleev's periodic table is an empirically supported scheme which allows one to categorize the physical and chemical properties of the elements by linking them with the rule of the successive occupation of the atomic orbitals. With increasing the atomic number Z, relativistic effects grow substantially. They can significantly alter various properties of the elements as compared with their lighter homologues. A classical example of the relativistic effects is the yellow color of gold [1–3]. In the region of the superheavy elements (SHEs) belonging to the seventh period of the table, the interplay between the relativistic and electron-electron correlation effects gives rise to the trends of deviation from the periodic law [4–8]. Some of these deviations, such as a different ground-state configuration of Lr ($Z = 103$) relative to its lighter homologue Lu ($Z = 71$), are confirmed experimentally [9]; others, like a positive electron affinity in Og ($Z = 118$), are predicted only theoretically [10–14]. Whether the eighth-period SHEs (with $Z > 118$) fit the periodic table and obey the periodic law is an open, intriguing question. For instance, this period brings into play the previously-never-met $5g$ shell, and the corresponding electronic-structure feature no doubt must be presented in possible extensions of the periodic table. In addition, the influence of the quantum-electrodynamics (QED) effects on the SHE ground states has not been investigated systematically so far.

A review of the current status of the problem and an extension of the periodic table up to $Z = 172$ based on the Dirac-Fock (DF) calculations, also known as the relativistic Hartree-Fock ones, are presented in Ref. [15], see also a very recent review [16]. This upper bound is determined by the fact that at higher values of Z the lowest (1s) Dirac level "dives" into the negative-energy continuum, provided a reasonable model for the nuclear charge distribution is employed [17–28].

The key point for the description of the SHE properties is determination of the ground-state configuration. The first attempts to advance the study of the SHEs beyond the seventh period and to conjecture on their chemical and physical properties were undertaken in the 1970s [29–34]. Throughout the years, the issue was addressed by using various one-configuration methods [35,36]. It soon became clear that in many cases the total energies of various configurations differ very little from each other, and more sophisticated configuration-interaction calculations are necessary. Taking into account the correlation effects may lead to a change in the ground-state configuration.

Some SHEs from the eighth period were studied within the many-configuration approaches [37–46]. The only paper that went beyond the one-configuration approximation for all the eighth period elements is Ref. [47]. The multiconfiguration Dirac-Fock method was used there to account for the interaction between energetically close configurations in the SHEs with $Z \leqslant 164$. As a result, in about 50% of cases the ground-state configurations found in Ref. [47] differ from the ones obtained in the previous Dirac-Fock-Slater calculations [34], where no electron-electron correlation effects were considered. In Ref. [47], only the ground-state configurations were reported without any information on the level structure. The stability of the obtained results with respect to the accuracy of the correlation treatment was not discussed in that work as well.

There are also some other issues that need to be clarified when discussing the SHE ground states. Does the one-configuration description remain valid for such complex systems possessing quite a large number of valence shells with, in particular, the $5g$ one among them? In other words, it seems reasonable that the ground-state level of the SHEs generally cannot be found without taking into account the electron-correlation effects, but is it possible, in principle, to describe with sufficient accuracy this state using a single configuration? Can previously unaccounted QED effects change the ground state of the SHEs? The present paper aims to investigate these points in the framework of the relativistic Dirac-Fock method and the configuration-interaction method

in the basis of the Dirac-Fock-Sturm orbitals [48–50]. In our calculations, in order to investigate a possible influence of the QED effects on the electronic structure and the ground-state configuration, both methods are paired with the model-QED-operator approach [51,52], which has been recently extended to the region $120 \leqslant Z \leqslant 170$ in Ref. [53].

The paper is organized as follows. In Sec. II, an overview of the methods and their main implementation features are presented. The numerical details and the particular aspects of the calculation procedure are given in Sec. III. We discuss the obtained results and compare them with the previous calculations in Sec. IV. Section V concludes the paper with a brief summary.

Atomic units are used throughout the paper.

II. THEORETICAL APPROACHES AND METHODS

In the present work, to explore the SHE ground states we use the DF and configuration-interaction (CI) methods. The issue is studied from different perspectives using one- as well as many-configuration approaches.

We consider a relativistic configuration K defined by the occupation numbers $\{q_a\}_{a=1}^{N_s}$, where the index a enumerates the relativistic shells. For the list of the relativistic shells $(n_1 l_1 j_1)^{q_1} \ldots (n_{N_s} l_{N_s} j_{N_s})^{q_{N_s}}$ (n is the principal quantum number, l and j are the orbital and total angular momenta, respectively), we first determine the DF energy obtained within the relativistic-configuration-average (RAV) approximation, also known in the literature as the jj-average approximation [54]. The corresponding total DF energy can be formally written as

$$E_{\rm RAV}^{\rm DF}(K) = \frac{1}{N_d} \sum_{\alpha \in K} \langle \alpha | \hat{H}^{\rm DC} | \alpha \rangle, \tag{1}$$

where $\alpha \equiv \det_\alpha \{\varphi_i^{\rm DF}\}$ are the Slater determinants constructed from the one-electron DF orbitals $\varphi_i^{\rm DF}$ belonging to the configuration K, and N_d is the number of these determinants. $\hat{H}^{\rm DC}$ is the many-electron Dirac-Coulomb Hamiltonian,

$$\hat{H}^{\rm DC} = \Lambda^+ [\hat{H}^{\rm D} + \hat{V}^{\rm C}] \Lambda^+, \tag{2}$$

where $\hat{H}^{\rm D}$ is the sum of the one-electron Dirac Hamiltonians with the nuclear potential $V(r)$,

$$\hat{H}^{\rm D} = \sum_{i=1}^{N} [(\boldsymbol{\alpha}_i \cdot \boldsymbol{p}_i) c + (\beta - 1) mc^2 + V(r_i)], \tag{3}$$

$\hat{V}^{\rm C}$ is the Coulomb electron-electron interaction operator,

$$\hat{V}^{\rm C} = \frac{1}{2} \sum_{i \neq j}^{N} \frac{1}{r_{ij}}, \tag{4}$$

and Λ^+ is the product of one-electron projectors on the positive-energy solutions of the DF-RAV equations. Here and below the indices i and j enumerate the electrons, N is their number, $\boldsymbol{p}$ is the momentum operator, $\boldsymbol{r}$ is the electron position vector, $r_{ij} = \boldsymbol{r}_i - \boldsymbol{r}_j$, $r = |\boldsymbol{r}|$, and $\boldsymbol{\alpha}$ and β are the Dirac matrices. In the DF-RAV approximation, the summation in the functional (1), which can be performed analytically, is equivalent to the summation over the relativistic terms J of the configuration K, taking into account their multiplicities [55,56]. The DF equations can be derived by varying Eq. (1) with the evident constraints due to the orthonormality conditions. The DF orbitals $\varphi_i^{\rm DF}$ and the energy $E_{\rm RAV}^{\rm DF}(K)$ are then obtained by solving the corresponding DF equations. We note that only the Coulomb-interaction operator $\hat{V}_{\rm C}$ is included self-consistently into the DF equations.

The Breit-interaction correction to the average energy $E_{\rm RAV}^{\rm DF}(K)$ of the configuration K is evaluated perturbatively as

$$\Delta E_{\rm RAV}^{\rm B}(K) = \frac{1}{N_d} \sum_{\alpha \in K} \langle \alpha | \hat{V}^{\rm B} | \alpha \rangle, \tag{5}$$

where the determinants α are constructed from $\varphi_i^{\rm DF}$ and $\hat{V}^{\rm B}$ is the Breit-interaction operator,

$$\hat{V}^{\rm B} = -\frac{1}{2} \sum_{i \neq j}^{N} \frac{1}{2 r_{ij}} \left[\boldsymbol{\alpha}_i \cdot \boldsymbol{\alpha}_j + \frac{(\boldsymbol{\alpha}_i \cdot \boldsymbol{r}_{ij})(\boldsymbol{\alpha}_j \cdot \boldsymbol{r}_{ij})}{r_{ij}^2} \right]. \tag{6}$$

The QED corrections are treated using the model-QED-operator approach developed in Refs. [51,52]. The Uehling part of the vacuum-polarization contribution is described by the well-known local potential, which can easily be calculated for any nuclear-charge distribution density. Meanwhile, the Wichmann-Kroll part of the vacuum-polarization correction as well as the self-energy contribution are represented for the SHEs via the nonlocal potentials [53]. We also mention some alternative methods to approximately account for the QED effects in many-electron systems, see, e.g., Refs. [40,44,57–62]. For very recent applications and developments of the model-QED-operator methods, which include the calculations of the QED effects in molecules, we refer to Refs. [63–68]. Like the Breit-interaction contribution, the QED correction in the RAV approximation is calculated as the relativistic-configuration-average expectation value of the model-QED operator $\hat{V}^{\rm Q}$,

$$\Delta E_{\rm RAV}^{\rm Q}(K) = \frac{1}{N_d} \sum_{\alpha \in K} \langle \alpha | \hat{V}^{\rm Q} | \alpha \rangle. \tag{7}$$

Finally, for the configuration K, we consider the average energy including the Breit correction and QED effects,

$$E_{\rm RAV}^{\rm DCBQ}(K) = E_{\rm RAV}^{\rm DF}(K) + \Delta E_{\rm RAV}^{\rm B}(K) + \Delta E_{\rm RAV}^{\rm Q}(K). \tag{8}$$

Hereinafter, this scheme is referred to as the DCBQ-RAV one.

To resolve the level structure for the configuration K, one can try to find a single-configuration DF wave function and corresponding energy for the jj-coupling term using the energy functional constructed for a given value of J. However, if this approach is employed for an open-shell system possessing a complex level structure, it often proves impossible to adequately select a proper linear combination of many-electron wave functions solely from symmetry considerations. It turns out that most of the SHEs have several open shells, and therefore, this straightforward scheme may result in a wrong level structure. In the present work, the level structure of the configuration K is resolved by means of the CI approach for the Dirac-Coulomb-Breit (DCB) Hamiltonian supplemented with the model-QED operator. The DCBQ Hamiltonian reads as

$$\hat{H}^{\rm DCBQ} = \Lambda^+ [\hat{H}^{\rm D} + \hat{V}^{\rm C} + \hat{V}^{\rm B} + \hat{V}^{\rm Q}] \Lambda^+, \tag{9}$$

where the operators Λ^+ are defined as in Eq. (2). The eigenvalue problem induced by the Hamiltonian (9) in the space of all the determinants α arising from the single relativistic configuration (SRC) K describes the splitting of the levels,

$$\hat{H}^{\mathrm{DCBQ}}\Psi_{\mathrm{SRC}}(K, JM) = E^{\mathrm{DCBQ}}_{\mathrm{SRC}}\Psi_{\mathrm{SRC}}(K, JM), \tag{10}$$

where

$$\Psi_{\mathrm{SRC}}(K, JM) = \sum_{\alpha\in K} C^{K,JM}_{\alpha}\det{}_{\alpha}\{\varphi^{\mathrm{DF}}_i\}, \tag{11}$$

with M being the projection of J.

However, in the case of energetically close configurations, their strong interaction and mixing may result in changes of the level structure. To account for the correlation effects, we consider a larger CI problem,

$$\hat{H}^{\mathrm{DCBQ}}\Psi_{\mathrm{CI}}(JM) = E^{\mathrm{DCBQ}}_{\mathrm{CI}}(J)\Psi_{\mathrm{CI}}(JM), \tag{12}$$

in the space spanned by the Slater determinants generated not from the single configuration K but from a given list of relativistic configurations $\{K_j\}_{j=1}^{N_c}$ (see details in the next section):

$$\Psi_{\mathrm{CI}}(JM) = \sum_{\alpha\in\{K_j\}_{j=1}^{N_c}} C^{JM}_{\alpha}\det{}_{\alpha}\{\varphi^{\mathrm{DF}}_i\}. \tag{13}$$

In the present calculations, the CI method in the basis of the Dirac-Fock-Sturm orbitals is used (CI-DFS) [48–50]. At the CI level, the Breit and QED corrections are taken into account, according to Eqs. (9)–(12), by including the corresponding terms into the Dirac-Coulomb Hamiltonian.

Finally, we emphasize that the main goal of the present study is not to obtain the most accurate theoretical predictions for the SHE energy-level structure, since in the cases of complex configurations this can be a separate, extremely complicated task. Instead, we aim at a reliable determination of the ground-state levels and the configurations they belong to within a series of the adequate relativistic calculations.

Having discussed the methods, let us proceed to details of their application in the scope of the present work.

III. DETAILS OF THE CALCULATIONS

In the present work, all the calculations of the energy levels of SHE are performed employing the Fermi model for the nuclear-charge distribution. The root-mean-square radius of the nucleus (in fermi) is given by

$$R = \sqrt{\frac{3}{5}}R_{\mathrm{sphere}}, \quad R_{\mathrm{sphere}} = 1.2A^{1/3}, \tag{14}$$

where for the nucleon number A we use the approximate formula from Ref. [20],

$$A = 0.00733Z^2 + 1.30Z + 63.6. \tag{15}$$

The value of A obtained from Eq. (15) is rounded to the nearest integer. This choice of the nuclear size is consistent with the one made in Ref. [53].

The SHE ground-state configuration is *a priori* unknown. As described in the previous section, we use three schemes to define the ground-state configuration. The first scheme is based on the DF-RAV method. Probing various configurations K, we determine the ground-state one as the configuration K^* with the lowest average energy $E^{\mathrm{DCBQ}}_{\mathrm{RAV}}(K^*)$. For each Z, the list of all possible configuration candidates for the role of the ground one is constructed by distributing $N_e = Z - N_{\mathrm{core}}$ valence electrons over the valence relativistic shells. The number of core-shell electrons N_{core} and the list of valence shells are presented in Table I. We consider as the valence shells those which, according to our preliminary calculations, are most likely to be occupied in the ground state.

TABLE I. List of the relativistic shells used to generate the relativistic configurations for which the DF-RAV equations are solved. The absence of the lower index j in the column "Core shells" means that all relativistic orbitals corresponding to the nonrelativistic one are fully occupied. The probe configurations are generated according to the following rule: The core shells are fully occupied, and the $Z - N_{\mathrm{core}}$ valence electrons are distributed over the valence shells. The notations [Rn] and [Og] represent the closed-shell configurations of radon and oganesson atoms, respectively.

Z	Core shells	N_{core}	Valence shells
120–121	[Rn]$5f\,6d\,7s\,7p_{1/2}$	114	$7p_{3/2}\,8s\,8p_{1/2}\,7d_{3/2}$
122–123	[Og]	118	$8s\,8p_{1/2}\,7d_{3/2}\,6f_{5/2}$
124–133	[Og]$8s$	120	$8p_{1/2}\,6f_{5/2}\,7d_{3/2}\,5g_{7/2}$
134–144	[Og]$8s\,5g_{7/2}$	128	$8p_{1/2}\,6f_{5/2}\,7d_{3/2}\,5g_{9/2}$
145–146	[Og]$8s\,8p_{1/2}\,5g_{7/2}$	130	$6f_{5/2}\,7d_{3/2}\,5g_{9/2}\,9s$
147–155	[Og]$8s\,8p_{1/2}\,5g$	140	$6f_{5/2}\,7d_{3/2}\,6f_{7/2}\,9s$
156–160	[Og]$8s\,8p_{1/2}\,5g\,6f_{5/2}$	146	$6f_{7/2}\,7d_{3/2}\,9s\,7d_{5/2}$
161–165	[Og]$8s\,8p_{1/2}\,5g\,6f$	154	$7d_{3/2}\,7d_{5/2}\,9s\,8p_{3/2}$
166–168	[Og]$8s\,8p_{1/2}\,5g\,6f\,7d_{3/2}$	158	$7d_{5/2}\,9s\,8p_{3/2}\,9p_{1/2}$
169–170	[Og]$8s\,8p_{1/2}\,5g\,6f\,7d$	164	$9s\,8p_{3/2}\,9p_{1/2}\,7f_{5/2}$

As an example, in Table II for the SHEs with $Z = 125$ and $Z = 140$, seven configurations K with the lowest relativistic-configuration-average energies $E^{\mathrm{DF}}_{\mathrm{RAV}}(K)$ are presented. For each configuration K given relative to the closed-shell one, the total DF-RAV energy and the energies obtained by successively adding the Breit and QED corrections are placed in the fourth, fifth, and sixth columns of Table II, respectively. The configurations are sorted in ascending order of the energy $E^{\mathrm{DF}}_{\mathrm{RAV}}(K)$, i.e., the first entry corresponds to the configuration with the lowest energy. The relative changes in the order of the configurations after addition of the corrections are indicated by the symbols $\triangledown$ (down) and $\triangle$ (up). The absence of these symbols corresponds to the case when the configuration position in the sorted list does not change.

As one can see from the examples given in Table II, the Breit-interaction correction can change the ground-state configuration within the RAV approximation. For $Z = 125$, Table II demonstrates that when only the Coulomb interaction is taken into account, the ground-state configuration is $8p^1_{1/2}6f^4_{5/2}$. However, when we add the Breit-interaction correction evaluated according to Eq. (5), the configuration $8p^1_{1/2}6f^3_{5/2}5g^1_{7/2}$ turns out to be the lowest-energy one. All six other configurations change their order as well. A similar configuration reordering occurs for the SHE with $Z = 140$. However, in the latter case some configurations retain their positions. Without the Breit interaction, the ground-state configuration for $Z = 140$ is $7d^2_{3/2}6f^2_{5/2}5g^6_{9/2}$, but with this correction taken into account the lowest-energy configuration

TABLE II. The relativistic-configuration-average energies for the SHEs with $Z = 125$ and $Z = 140$ evaluated for the configurations K using the DF method, $E^{\rm DF}_{\rm RAV}$, with the addition of the Breit-interaction correction, $+\Delta E^{\rm B}_{\rm RAV}$, and with the additional accounting for the QED correction, $+\Delta E^{\rm Q}_{\rm RAV}$ (a.u.). The configurations are presented relative to the closed-shell configuration and sorted in the ascending order of the energy $E^{\rm DF}_{\rm RAV}$. In the last two columns, the symbols ▽ (down) and △ (up) indicate the change in the order of the configurations relative to the order in the preceding column. The absence of these symbols means that there is no change in the position of the configuration. In particular, the QED effects do not affect the order.

Z	Closed shells	K	$E^{\rm DF}_{\rm RAV}$	$+\Delta E^{\rm B}_{\rm RAV}$	$+\Delta E^{\rm Q}_{\rm RAV}$
125	$[{\rm Og}]8s^2_{1/2}$	$8p^1_{1/2}6f^4_{5/2}$	−64 846.3116	−64 718.7639 ▽3	−64 627.5323
		$8p^1_{1/2}6f^3_{5/2}5g^1_{7/2}$	−64 846.3061	−64 718.7781 △1	−64 627.5496
		$8p^1_{1/2}7d^1_{3/2}6f^2_{5/2}5g^1_{7/2}$	−64 846.3033	−64 718.7718 △1	−64 627.5421
		$8p^2_{1/2}6f^2_{5/2}5g^1_{7/2}$	−64 846.3007	−64 718.7680 △1	−64 627.5377
		$7d^1_{3/2}6f^4_{5/2}$	−64 846.2769	−64 718.7300 ▽1	−64 627.4988
		$8p^1_{1/2}7d^1_{3/2}6f^3_{5/2}$	−64 846.2697	−64 718.7182 ▽1	−64 627.4854
		$7d^1_{3/2}6f^3_{5/2}5g^1_{7/2}$	−64 846.2680	−64 718.7408 △2	−64 627.5127
140	$[{\rm Og}]8s^2_{1/2}8p^2_{1/2}5g^8_{7/2}$	$7d^2_{3/2}6f^2_{5/2}5g^6_{9/2}$	−93 548.8504	−93 320.7516 ▽1	−93 179.0799
		$7d^1_{3/2}6f^3_{5/2}5g^6_{9/2}$	−93 548.8479	−93 320.7539 △1	−93 179.0837
		$7d^1_{3/2}6f^4_{5/2}5g^5_{9/2}$	−93 548.7928	−93 320.6719 ▽1	−93 178.9986
		$7d^3_{3/2}6f^1_{5/2}5g^6_{9/2}$	−93 548.7738	−93 320.6697 ▽1	−93 178.9965
		$6f^4_{5/2}5g^6_{9/2}$	−93 548.7689	−93 320.6791 △2	−93 179.0103
		$6f^5_{5/2}5g^5_{9/2}$	−93 548.7559	−93 320.6398	−93 178.9679
		$7d^2_{3/2}6f^3_{5/2}5g^5_{9/2}$	−93 548.7488	−93 320.6229	−93 178.9480

is $7d^1_{3/2}6f^3_{5/2}5g^6_{9/2}$. For both demonstrated cases, the QED correction does not change the ground-state configuration and the sorted configuration list as a whole.

After the configurations with the lowest average energies $E^{\rm DCBQ}_{\rm RAV}(K)$ are found, we explore their level structure using the DCBQ-SRC approach. To determine the ground-state level, we choose seven configurations with the lowest DCBQ-RAV energies and for each level belonging to these configurations solve the DCBQ-SRC problem (10). The configuration with the lowest DCBQ-SRC energy is considered to be the ground-state configuration in the DCBQ-SRC approach, and the corresponding level gives the ground-state level. Since for most SHEs a few selected DCBQ-RAV energies are close to each other, we bear in mind that the DCBQ-SRC consideration can change the ground-state configuration.

The last statement is illustrated in Fig. 1, where the average energies $E^{\rm DCBQ}_{\rm RAV}(K)$ of the SHE with $Z = 125$ are presented for two configurations having the lowest DCBQ-RAV energies: $K = 8p^1_{1/2}6f^3_{5/2}5g^1_{7/2}$ (left) and $\tilde{K} = 8p^1_{1/2}7d^1_{3/2}6f^2_{5/2}5g^1_{7/2}$ (right). For each configuration, we show all the levels $E^{\rm DCBQ}_{\rm SRC}(K, J)$ contributing to the relativistic-configuration-average energy. For the lowest DCBQ-SRC levels, the total angular momenta J are presented. One can see, that the average energy of the configuration K is lower than the energy of the configuration $\tilde{K}$ by about $E^{\rm DCBQ}_{\rm RAV}(\tilde{K}) - E^{\rm DCBQ}_{\rm RAV}(K) = 0.0075$ a.u. (see also Table II). However, the lowest level $J = 17/2$ of the configuration $\tilde{K}$ lies lower than the lowest level $J = 13/2$ of the configuration K by about $E^{\rm DCBQ}_{\rm SRC}(K, 13/2) - E^{\rm DCBQ}_{\rm SRC}(\tilde{K}, 17/2) = 0.0245$ a.u. This kind of behavior is not a specific feature of the SHE with $Z = 125$, but rather an example of some general trend observed for many other SHEs as well.

The DCBQ-RAV and DCBQ-SRC schemes are one-configuration approaches and therefore they do not take into account the electron-correlation effects, i.e., mixing of the different configurations. Below, we discuss the influence of the electron-electron correlations on the order of the SHE lowest levels. To this end, for each Z we perform the independent CI-DFS calculations for seven reference configurations with the lowest DCBQ-RAV energies selected at the previous

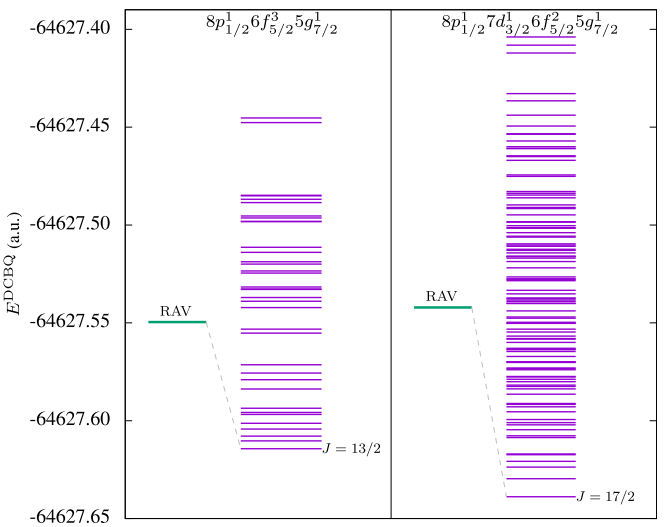

FIG. 1. Relativistic-configuration-average energies $E^{\rm DCBQ}_{\rm RAV}$ calculated for the configurations $8p^1_{1/2}6f^3_{5/2}5g^1_{7/2}$ (left) and $8p^1_{1/2}7d^1_{3/2}6f^2_{5/2}5g^1_{7/2}$ (right) of the SHE with $Z = 125$ and all the possible levels which contribute to these average energies. For the lowest DCBQ-SRC levels the total angular momentum quantum numbers J are shown.

TABLE III. The list of the active and virtual relativistic shells employed in the DCBQ-CI1 and DCBQ-CI2 calculations. The absence of the lower index indicates that for a given l both the relativistic orbitals with $l - 1/2$ and $l + 1/2$ are included in the CI problem.

		Virtual shells	
Z	Active valence shells	DCBQ-CI1	DCBQ-CI2
120–121	$7p_{3/2}8s_{1/2}8p_{1/2}7d_{3/2}$	$8p_{3/2}7d_{5/2}$	$9s_{1/2}9p8d6f5g$
122–123	$8s_{1/2}8p_{1/2}7d_{3/2}6f_{5/2}$	$8p_{3/2}7d_{5/2}6f_{7/2}$	$9s_{1/2}9p8d7f5g$
124–133	$8p_{1/2}6f_{5/2}7d_{3/2}5g_{7/2}$	$8p_{3/2}7d_{5/2}6f_{7/2}5g_{9/2}$	$9s_{1/2}9p8d7f6g$
134–144	$8p_{1/2}6f_{5/2}7d_{3/2}5g_{9/2}$	$8p_{3/2}6f_{7/2}7d_{5/2}$	$9s_{1/2}9p_{1/2}8d_{3/2}7f_{5/2}6g_{7/2}$
145–146	$6f_{5/2}7d_{3/2}5g_{9/2}9s_{1/2}$	$8p_{3/2}6f_{7/2}7d_{5/2}$	$10s_{1/2}9p8d7f6g$
147–155	$6f_{5/2}7d_{3/2}6f_{7/2}9s_{1/2}$	$8p_{3/2}7d_{5/2}$	$10s_{1/2}9p8d7f6g$
156–160	$6f_{7/2}7d_{3/2}9s_{1/2}7d_{5/2}$	$8p_{3/2}$	$10s_{1/2}9p8d7f6g$
161–165	$7d_{3/2}7d_{5/2}9s_{1/2}8p_{3/2}$		$10s_{1/2}9p8d7f6g$
166–168	$7d_{3/2}7d_{5/2}9s_{1/2}8p_{3/2}9p_{1/2}$	$9p_{3/2}$	$10s_{1/2}10p8d7f6g$
169–170	$7d_{5/2}9s_{1/2}8p_{3/2}9p_{1/2}7f_{5/2}$	$7f_{7/2}9p_{3/2}$	$10s_{1/2}10p8d8f6g$

stage. For each configuration, we evaluate the three lowest levels and determine their total angular momenta J. The level with the lowest energy $E_{\rm CI}^{\rm DCBQ}(J)$ is the ground-state level. Within this approach, the ground-state level depends on how accurately we solve the CI problem. We investigate the dependence of the level order on the number of virtual orbitals by performing two different CI-DFS calculations, referred to as "DCBQ-CI1" and "DCBQ-CI2." In both schemes, the single (S) and double (D) excitations from the reference configuration determined at the DCBQ-RAV stage are considered. The DCBQ-CI1 scheme can be thought of as a CI problem with a relatively small number of virtual orbitals, whereas the DCBQ-CI2 scheme includes more virtual orbitals. The list of the active and virtual orbitals used in both CI calculations is presented in Table III. The occupied orbitals, which are not mentioned in the table, are treated as the frozen core. The active orbitals as well as the virtual orbitals, which are involved in the most important configurations, are taken as the solutions of the DF equations, whereas the other virtual orbitals are obtained from the solutions of the DFS equations.

The correlation effects can result in exotic scenarios for the level structure. An example is presented in Table IV, where the lowest levels with $J = 0, 1, 2, 3$ and the related configurations of the SHE with $Z = 168$ are shown. One can see that within the DCBQ-SRC approximation, when the electron-electron correlations are neglected, the level with $J = 1$, $E_{\rm SRC}^{\rm DCBQ}(J = 1) = -202\,904.8013$ a.u., lies below the levels with $J = 2$, $E_{\rm SRC}^{\rm DCBQ}(J = 2) = -202904.7871$ a.u. and $J = 0$, $E_{\rm SRC}^{\rm DCBQ}(J = 0) = -202\,904.7789$ a.u. If we account for the electronic correlations by means of the DCBQ-CI1 scheme, the level with $J = 1$ rises above the level with $J = 2$ and exceeds it by about 0.025 a.u. When we improve the description of the electron-electron correlations using the DCBQ-CI2 scheme, the level with $J = 1$ becomes the lowest one again and the level with $J = 0$ falls below the level with $J = 2$. In this case, the difference between the levels with $J = 0$ and $J = 1$ constitutes about 0.01 a.u. This demonstrates that with the improvement of the correlation treatment, changes in the ground-state levels may occur. More importantly, the dominant configurations of levels with $J = 0, 1, 2$ do not coincide with each other. Therefore, one can expect that not only levels which belong to the same configuration can interchange, but also the rearrangements involving the levels of other configurations are possible.

TABLE IV. The lowest-level energies $E^{\rm DCBQ}(J)$ for levels $J = 0, 1, 2, 3$ calculated by means of DCBQ-SRC, DCBQ-CI1, and DCBQ-CI2 schemes for the SHE with $Z = 168$ (a.u.). For the DCBQ-SRC values, the configurations of these levels are presented. For the DCBQ-CI1 and DCBQ-CI2 results, the configurations contributing with weights of at least 0.05 are given.

	DCBQ-SRC		DCBQ-CI1		DCBQ-CI2	
J	K	$E_{\rm SRC}^{\rm DCBQ}(K, J)$	K	$E_{\rm CI}^{\rm DCBQ}(J)$	K	$E_{\rm CI}^{\rm DCBQ}(J)$
0	$9s_{1/2}^2 9p_{1/2}^2$	−202 904.7789	$0.87 \times 9s_{1/2}^2 9p_{1/2}^2 +$ $0.07 \times 9s_{1/2}^2 8p_{3/2}^2 +$ $0.05 \times 8p_{3/2}^2 9p_{1/2}^2$	−202 904.8206	$0.91 \times 9s_{1/2}^2 9p_{1/2}^2$	−202 904.9561
1	$9s_{1/2}^2 8p_{3/2}^1 9p_{1/2}^1$	−202 904.8013	$0.92 \times 9s_{1/2}^2 8p_{3/2}^1 9p_{1/2}^1 +$ $0.07 \times 8p_{3/2}^3 9p_{1/2}^1$	−202 904.8247	$0.94 \times 9s_{1/2}^2 8p_{3/2}^1 9p_{1/2}^1$	−202 904.9652
2	$9s_{1/2}^1 8p_{3/2}^2 9p_{1/2}^1$	−202 904.7871	$0.55 \times 9s_{1/2}^1 8p_{3/2}^2 9p_{1/2}^1 +$ $0.24 \times 9s_{1/2}^1 8p_{3/2}^1 9p_{1/2}^2 +$ $0.20 \times 9s_{1/2}^1 8p_{3/2}^3$	−202 904.8491	$0.81 \times 9s_{1/2}^1 8p_{3/2}^2 9p_{1/2}^1 +$ $0.09 \times 9s_{1/2}^1 8p_{3/2}^1 9p_{1/2}^2 +$ $0.07 \times 9s_{1/2}^1 8p_{3/2}^3$	−202 904.9542
3	$9s_{1/2}^1 8p_{3/2}^2 9p_{1/2}^1$	−202 904.7319	$0.99 \times 9s_{1/2}^1 8p_{3/2}^2 9p_{1/2}^1$	−202 904.7385	$0.96 \times 9s_{1/2}^1 8p_{3/2}^2 9p_{1/2}^1$	−202 904.8835

IV. RESULTS

To begin with, we calculate the average energies of the configurations including the Breit interaction and QED effects within the DCBQ-RAV method. For all the SHEs in the range $120 \leqslant Z \leqslant 170$, the configurations with the lowest average energy are presented in Table V. The ground-state configurations are shown relative to the closed-shell configurations given in the second column. Our results (the column "DCBQ-RAV") are compared with the results of Ref. [34], where the calculations were performed using the Dirac-Fock-Slater method for Z up to 173; the results of Ref. [29], where the DF method was employed for Z up to 131; and, finally, the results of Ref. [35], where the calculations were based on the relativistic density functional theory and $121 \leqslant Z \leqslant 131$ were considered. We note that in Ref. [29] the Gaunt-interaction correction was taken into account perturbatively, while the Coulomb electron-electron interaction was treated self-consistently within the density functional theory. Moreover, since nonrelativistic notations were used in Refs. [29,35], we retain them in Table V without any changes.

Within the DCBQ-RAV approximation, the general trend of the occupation rule with the growth of Z is as follows: after the $8s_{1/2}$ shell is filled for $Z = 120$, the electrons begin to occupy the $8p_{1/2}$, $7d_{3/2}$, and $6f_{5/2}$ shells. According to our calculations, the first electron in the $5g_{7/2}$ shell appears for $Z = 125$. Starting from this atomic number, the $5g$ series begins. For $Z = 126$, the $8p_{1/2}$ shell becomes the closed one. With a further increase for Z, the $5g_{7/2}$ and $5g_{9/2}$ shells are subsequently occupied with the electrons. The partially occupied $7d_{3/2}$ and $6f_{5/2}$ shells remain the valence ones and their occupation numbers exhibit little changes. This $5g$-occupation process is completed at $Z = 144$ which has the fully occupied $5g_{7/2}$ and $5g_{9/2}$ shells and partially occupied $7d_{3/2}$ and $6f_{5/2}$ shells.

After both the relativistic $5g$ shells are filled, the $6f$ shells begin to be occupied quite systematically: $6f_{5/2}$ and $6f_{7/2}$ become fully occupied for $Z = 148$ and $Z = 155$, respectively. The $7d_{3/2}$ shell is unoccupied for $Z = 155$ and it remains partially occupied for the other Z in this region becoming closed only for $Z = 158$. Finally, the SHE with $Z = 164$ has the configuration $[\mathrm{Og}]8s^2_{1/2}8p^2_{1/2}5g^8_{7/2}5g^{10}_{9/2}6f^6_{5/2}6f^8_{7/2}7d^4_{3/2}7d^6_{5/2}$, with all the relativistic shells being occupied.

Notably, the $8p_{3/2}$ shell is not filled along the sequence $Z = 120 - 166$ that is due to a large spin-orbital splitting of the $8p$ shell. The DF-RAV calculations for $Z = 166$ shows that the spin-orbital splitting of the $8p$ shell is about 80 eV. The first $8p_{3/2}$ electron appears in the SHE with $Z = 167$, after the $9s_{1/2}$ shell becomes the closed one. However, for $Z = 168$ the $9p_{1/2}$ shell turns out to be more energetically advantageous than the $8p_{3/2}$ one. The $8p_{3/2}$ shell is not fully occupied even for the last considered SHE with $Z = 170$. Another remarkable observation found in our DCBQ-RAV calculations is that for $Z = 155$ the configuration with the valence $9s_{1/2}$ electron turn out to be more energetically beneficial than the configuration with $7d_{3/2}$ electrons, whereas its neighbors $Z = 154$ and $Z = 156$ have two electrons in the $7d_{3/2}$ shell. Next time the $9s_{1/2}$ electron appears in the series $Z = 159 - 161$, and, finally, the $9s_{1/2}$ shell establishes on the regular basis starting from the element with $Z = 165$.

Throughout the calculations we found that the ground-state configuration may change due to the Breit-interaction corrections, see the discussion in Sec. III. This kind of change is observed for $Z = 125$ and $Z = 140$ and never occurs for other values of Z. This behavior can be explained as follows. For a given Z, the Breit-interaction contribution to the relative energies of the configurations under consideration may be of a different sign, depending on the competition between two opposing effects. Namely, a better localization of the valence electron not only directly increases its Breit-interaction energy with the other electrons, but also leads to a stronger screening of the nucleus, which indirectly decreases the Breit contribution for the rest of the electrons. Whether or not the ground-state configuration changes also depends on the differences between the total DF-RAV energies for the configurations with the lowest energies. The SHEs with $Z = 125$ and $Z = 140$ represent the cases where the smallness of the DF-RAV energy differences and the coming into play of the more localized electrons make the corresponding configurations more energetically favorable. Concerning the QED corrections, we deduce that within the DCBQ-RAV approach they never change the ground-state configuration for the SHEs under consideration. In general, our DCBQ-RAV ground-state configurations coincide with the DF-RAV ones, obtained without the Breit and QED corrections, in all cases except for $Z = 125$ and $Z = 140$.

Our DCBQ-RAV results for $Z = 120 - 131$ are in full agreement with the results of Ref. [29]. The obtained ground-state configurations agree with the related results of Ref. [35] for the SHEs with $Z = 121$ and $Z = 123$, but differ for the other available values of Z. Our DF-RAV results differ from the results of Ref. [34] obtained without the Breit and QED corrections for eight of the considered SHEs, namely, for $Z = 125$, 126, 132, 139, 140, 155, 167, and 168. For $Z = 155$, our results predict that the $9s_{1/2}$ electron unexpectedly jumps in the $6f_{7/2}$-occupation sequence. Perhaps the configuration with the valence $9s_{1/2}$ electron was not considered in Ref. [34]. As for the other discrepancies, they seem to have a nonsystematical nature and might be due to the Slater exchange-interaction approximation used in Ref. [34]. Nevertheless, the real reasons for these deviations remain unclear to us.

Proceeding with the analysis, we are aimed at finding the configuration of the lowest-energy level. We employ the CI-DFS method using the one-configuration scheme DCBQ-SRC as well as the more elaborated schemes DCBQ-CI1 and DCBQ-CI2. As in the DCBQ-RAV approach, in these schemes the Breit and QED corrections are included, however, in the nonperturbative manner. The thorough description of the CI calculations is presented in Sec. III.

In Table VI, we give the levels with the lowest DCBQ energies for the SHEs with $120 \leqslant Z \leqslant 170$ obtained in three considered CI schemes. Additionally, the quantum numbers J of these levels are listed. For the DCBQ-SRC results, the configurations which the ground-state levels belong to are given. The DCBQ-CI1 and DCBQ-CI2 results include the electron-electron correlation effects. For these data, we list the configurations contributing to the ground levels with a weight of at least 0.05. Following the structure of the previous table, the configurations are given relative to the closed-shell ones. The obtained results are compared with the results of

TABLE V. The ground-state configurations of superheavy elements with atomic numbers $120 \leqslant Z \leqslant 170$ evaluated within the DCBQ-RAV method, taking into account the Breit interaction and QED effects. The configurations are shown relative to the closed-shell ones, which are presented in the column "Closed shells." [Og] corresponds to the configuration of the oganesson atom. The succeeding records in this column show the relativistic orbitals which have to be added to the previous ones to obtain the closed-shell configurations for heavier atoms. The results of the present work, DCBQ-RAV, are compared with the results of Refs. [29,34,35].

Z	Closed shells	DCBQ-RAV	Fricke and Soff [34]	Mann and Waber [29]	Umemoto and Saito [35]
120	[Og]	$8s^2_{1/2}$	$8s^2_{1/2}$	$8s^2$	
121	$+8s^2_{1/2}$	$8p^1_{1/2}$	$8p^1_{1/2}$	$8p^1$	$8p^1$
122		$8p^1_{1/2}\ 7d^1_{3/2}$	$8p^1_{1/2}\ 7d^1_{3/2}$	$8p^1 7d^1$	$8p^2$
123		$8p^1_{1/2}\ 7d^1_{3/2}\ 6f^1_{5/2}$	$8p^1_{1/2}\ 7d^1_{3/2}\ 6f^1_{5/2}$	$8p^1 7d^1 6f^1$	$8p^1 7d^1 6f^1$
124		$8p^1_{1/2}\ 6f^3_{5/2}$	$8p^1_{1/2}\ 6f^3_{5/2}$	$8p^1 6f^3$	$8p^2 6f^2$
125		$8p^1_{1/2}\ 6f^3_{5/2}\ 5g^1_{7/2}$	$8p^1_{1/2}\ 6f^3_{5/2}\ 5g^1_{7/2}$	$8p^1 6f^3 5g^1$	$8p^1 6f^4$
126		$8p^2_{1/2}\ 6f^2_{5/2}\ 5g^2_{7/2}$	$8p^1_{1/2}\ 7d^1_{3/2}\ 6f^2_{5/2}\ 5g^2_{7/2}$	$8p^2 6f^2 5g^2$	$8p^1 6f^4 5g^1$
127	$+8p^2_{1/2}$	$6f^2_{5/2}\ 5g^3_{7/2}$	$6f^2_{5/2}\ 5g^3_{7/2}$	$8p^2 6f^2 5g^3$	$8p^2 6f^3 5g^2$
128		$6f^2_{5/2}\ 5g^4_{7/2}$	$6f^2_{5/2}\ 5g^4_{7/2}$	$8p^2 6f^2 5g^4$	$8p^2 6f^3 5g^3$
129		$6f^2_{5/2}\ 5g^5_{7/2}$	$6f^2_{5/2}\ 5g^5_{7/2}$	$8p^2 6f^2 5g^5$	$8p^2 6f^3 5g^4$
130		$6f^2_{5/2}\ 5g^6_{7/2}$	$6f^2_{5/2}\ 5g^6_{7/2}$	$8p^2 6f^2 5g^6$	$8p^2 6f^3 5g^5$
131		$6f^2_{5/2}\ 5g^7_{7/2}$	$6f^2_{5/2}\ 5g^7_{7/2}$	$8p^2 6f^2 5g^7$	$8p^2 6f^3 5g^6$
132		$7d^1_{3/2}\ 6f^1_{5/2}\ 5g^8_{7/2}$	$6f^2_{5/2}\ 5g^8_{7/2}$		
133	$+5g^8_{7/2}$	$6f^3_{5/2}$	$6f^3_{5/2}$		
134		$6f^4_{5/2}$	$6f^4_{5/2}$		
135		$6f^4_{5/2}\ 5g^1_{9/2}$	$6f^4_{5/2}\ 5g^1_{9/2}$		
136		$6f^4_{5/2}\ 5g^2_{9/2}$	$6f^4_{5/2}\ 5g^2_{9/2}$		
137		$7d^1_{3/2}\ 6f^3_{5/2}\ 5g^3_{9/2}$	$7d^1_{3/2}\ 6f^3_{5/2}\ 5g^3_{9/2}$		
138		$7d^1_{3/2}\ 6f^3_{5/2}\ 5g^4_{9/2}$	$7d^1_{3/2}\ 6f^3_{5/2}\ 5g^4_{9/2}$		
139		$7d^1_{3/2}\ 6f^3_{5/2}\ 5g^5_{9/2}$	$7d^2_{3/2}\ 6f^2_{5/2}\ 5g^5_{9/2}$		
140		$7d^1_{3/2}\ 6f^3_{5/2}\ 5g^6_{9/2}$	$7d^1_{3/2}\ 6f^3_{5/2}\ 5g^6_{9/2}$		
141		$7d^2_{3/2}\ 6f^2_{5/2}\ 5g^7_{9/2}$	$7d^2_{3/2}\ 6f^2_{5/2}\ 5g^7_{9/2}$		
142		$7d^2_{3/2}\ 6f^2_{5/2}\ 5g^8_{9/2}$	$7d^2_{3/2}\ 6f^2_{5/2}\ 5g^8_{9/2}$		
143		$7d^2_{3/2}\ 6f^2_{5/2}\ 5g^9_{9/2}$	$7d^2_{3/2}\ 6f^2_{5/2}\ 5g^9_{9/2}$		
144		$7d^3_{3/2}\ 6f^1_{5/2}\ 5g^{10}_{9/2}$	$7d^3_{3/2}\ 6f^1_{5/2}\ 5g^{10}_{9/2}$		
145	$+5g^{10}_{9/2}$	$7d^2_{3/2}\ 6f^3_{5/2}$	$7d^2_{3/2}\ 6f^3_{5/2}$		
146		$7d^2_{3/2}\ 6f^4_{5/2}$	$7d^2_{3/2}\ 6f^4_{5/2}$		
147		$7d^2_{3/2}\ 6f^5_{5/2}$	$7d^2_{3/2}\ 6f^5_{5/2}$		
148		$7d^2_{3/2}\ 6f^6_{5/2}$	$7d^2_{3/2}\ 6f^6_{5/2}$		
149	$+6f^6_{5/2}$	$7d^3_{3/2}$	$7d^3_{3/2}$		
150		$7d^4_{3/2}$	$7d^4_{3/2}$		
151		$7d^3_{3/2}\ 6f^2_{7/2}$	$7d^3_{3/2}\ 6f^2_{7/2}$		
152		$7d^3_{3/2}\ 6f^3_{7/2}$	$7d^3_{3/2}\ 6f^3_{7/2}$		
153		$7d^2_{3/2}\ 6f^5_{7/2}$	$7d^2_{3/2}\ 6f^5_{7/2}$		
154		$7d^2_{3/2}\ 6f^6_{7/2}$	$7d^2_{3/2}\ 6f^6_{7/2}$		
155		$9s^1_{1/2}\ 6f^8_{7/2}$	$7d^2_{3/2}\ 6f^7_{7/2}$		
156	$+6f^8_{7/2}$	$7d^2_{3/2}$	$7d^2_{3/2}$		
157		$7d^3_{3/2}$	$7d^3_{3/2}$		
158		$7d^4_{3/2}$	$7d^4_{3/2}$		
159	$+7d^4_{3/2}$	$9s^1_{1/2}$	$9s^1_{1/2}$		
160		$7d^1_{5/2}\ 9s^1_{1/2}$	$7d^1_{5/2}\ 9s^1_{1/2}$		
161		$7d^2_{5/2}\ 9s^1_{1/2}$	$7d^2_{5/2}\ 9s^1_{1/2}$		
162		$7d^4_{5/2}$	$7d^4_{5/2}$		
163		$7d^5_{5/2}$	$7d^5_{5/2}$		
164		$7d^6_{5/2}$	$7d^6_{5/2}$		
165	$+7d^6_{5/2}$	$9s^1_{1/2}$	$9s^1_{1/2}$		
166		$9s^2_{1/2}$	$9s^2_{1/2}$		
167	$+9s^2_{1/2}$	$8p^1_{3/2}$	$9p^1_{1/2}$		
168		$8p^1_{3/2}\ 9p^1_{1/2}$	$9p^2_{1/2}$		
169		$8p^1_{3/2}\ 9p^2_{1/2}$	$8p^1_{3/2}\ 9p^2_{1/2}$		
170		$8p^2_{3/2}\ 9p^2_{1/2}$	$8p^2_{3/2}\ 9p^2_{1/2}$		

TABLE VI. The levels with lowest total energies, the main configurations contributing to them, and the total angular momenta J evaluated by means of the DCBQ-SRC, DCBQ-CI1, and DCBQ-CI2 schemes for SHEs with the atomic numbers $120 \leqslant Z \leqslant 170$. For the DCBQ-CI1 and DCBQ-CI2 results, the configurations with weights of at least 0.05 are presented. The configurations obtained are given relative to the closed-shell configurations listed in the column "Closed shells." In the first column, the values of Z in bold indicate the cases when the ground-state configurations obtained within the DCBQ-RAV and DCBQ-SRC methods differ. In addition, the following notations around Z are adopted to assist the reader in navigation through the table. The underline "___" means that the ground-state J_{SRC} level evaluated using the DCBQ-SRC approach differs from the J_{CI1} one calculated by means of the DCBQ-CI1 approach, $J_{\mathrm{SRC}} \neq J_{\mathrm{CI1}}$. The left vertical line "| " signalizes that the configuration K_{SRC} which the ground-state SRC level belongs to differs from the dominant configuration K_{CI1} of the ground-state CI1 level, $K_{\mathrm{SRC}} \neq K_{\mathrm{CI1}}$. The overline "—" represents the fact that $J_{\mathrm{CI1}} \neq J_{\mathrm{CI2}}$. Finally, the right vertical line " |" stands for the case $K_{\mathrm{CI1}} \neq K_{\mathrm{CI2}}$. The obtained ground-state levels are compared with the results of Ref. [47]. The nonrelativistic notation of Ref. [47] are retained.

Z	Closed shells	DCBQ-SRC	J_{SRC}	DCBQ-CI1	J_{CI1}	DCBQ-CI2	J_{CI2}	Ref. [47]
120	[Og]	$8s^2_{1/2}$	0	$0.94 \times 8s^2_{1/2}$	0	$0.93 \times 8s^2_{1/2}$	0	$8s^2$
121		$8s^2_{1/2}8p^1_{1/2}$	1/2	$0.92 \times 8s^2_{1/2}8p^1_{1/2}$	1/2	$0.91 \times 8s^2_{1/2}8p^1_{1/2}$	1/2	$8s^28p^1$
122		$8s^2_{1/2}8p^1_{1/2}7d^1_{3/2}$	2	$0.85 \times 8s^2_{1/2}8p^1_{1/2}7d^1_{3/2}+$ $0.09 \times 8s^1_{1/2}8p^1_{1/2}7d^2_{3/2}$	2	$0.84 \times 8s^2_{1/2}8p^1_{1/2}7d^1_{3/2}+$ $0.07 \times 8s^1_{1/2}8p^1_{1/2}7d^2_{3/2}$	2	$7d^18p^1$
123		$8s^2_{1/2}8p^1_{1/2}7d^1_{3/2}6f^1_{5/2}$	9/2	$0.83 \times 8s^2_{1/2}8p^1_{1/2}7d^1_{3/2}6f^1_{5/2}+$ $0.14 \times 8s^1_{1/2}8p^1_{1/2}7d^2_{3/2}6f^1_{5/2}$	9/2	$0.82 \times 8s^2_{1/2}8p^1_{1/2}7d^1_{3/2}6f^1_{5/2}+$ $0.09 \times 8s^1_{1/2}8p^1_{1/2}7d^2_{3/2}6f^1_{5/2}$	9/2	$6f^28p^1$
|**124**	$+8s^2$	$8p^1_{1/2}7d^1_{3/2}6f^2_{5/2}$	6	$0.83 \times 8p^1_{1/2}6f^3_{5/2}+$ $0.10 \times 8p^1_{1/2}6f^2_{5/2}6f^1_{7/2}$	5	$0.85 \times 8p^1_{1/2}6f^3_{5/2}+$ $0.07 \times 8p^1_{1/2}6f^2_{5/2}6f^1_{7/2}$	5	$6f^28p^2$
125		$8p^1_{1/2}7d^1_{3/2}6f^2_{5/2}5g^1_{7/2}$	17/2	$0.96 \times 8p^1_{1/2}7d^1_{3/2}6f^2_{5/2}5g^1_{7/2}$	17/2	$0.94 \times 8p^1_{1/2}7d^1_{3/2}6f^2_{5/2}5g^1_{7/2}$	17/2	$0.81 \times 5g^16f^28p^2+$ $0.17 \times 5g^16f^17d^28p^1+$ $0.02 \times 6f^37d^18p^1$
126		$8p^1_{1/2}7d^1_{3/2}6f^2_{5/2}5g^2_{7/2}$	10	$0.93 \times 8p^1_{1/2}7d^1_{3/2}6f^2_{5/2}5g^2_{7/2}$	10	$0.92 \times 8p^1_{1/2}7d^1_{3/2}6f^2_{5/2}5g^2_{7/2}$	10	$0.998 \times 5g^26f^38p^1+$ $0.002 \times 5g^26f^28p^2$
127		$8p^1_{1/2}7d^1_{3/2}6f^2_{5/2}5g^3_{7/2}$	27/2	$0.95 \times 8p^1_{1/2}7d^1_{3/2}6f^2_{5/2}5g^3_{7/2}$	27/2	$0.94 \times 8p^1_{1/2}7d^1_{3/2}6f^2_{5/2}5g^3_{7/2}$	27/2	$0.88 \times 5g^36f^28p^2+$ $0.12 \times 5g^36f^17d^28p^1$
128		$8p^1_{1/2}7d^1_{3/2}6f^2_{5/2}5g^4_{7/2}$	14	$0.80 \times 8p^1_{1/2}7d^1_{3/2}6f^2_{5/2}5g^4_{7/2}+$ $0.14 \times 8p^1_{1/2}7d^1_{3/2}6f^2_{5/2}5g^3_{7/2}5g^1_{9/2}$	14	$0.81 \times 8p^1_{1/2}7d^1_{3/2}6f^2_{5/2}5g^4_{7/2}+$ $0.13 \times 8p^1_{1/2}7d^1_{3/2}6f^2_{5/2}5g^3_{7/2}5g^1_{9/2}$	14	$0.88 \times 5g^46f^28p^2+$ $0.12 \times 5g^46f^17d^28p^1$
129		$8p^1_{1/2}7d^1_{3/2}6f^3_{5/2}5g^4_{7/2}$	29/2	$0.93 \times 8p^1_{1/2}7d^1_{3/2}6f^3_{5/2}5g^4_{7/2}+$ $0.06 \times 8p^1_{1/2}7d^1_{3/2}6f^2_{5/2}5g^4_{7/2}6f^1_{7/2}$	29/2	$0.94 \times 8p^1_{1/2}7d^1_{3/2}6f^3_{5/2}5g^4_{7/2}$	29/2	$5g^46f^37d^18p^1$
130|		$8p^1_{1/2}7d^1_{3/2}6f^3_{5/2}5g^5_{7/2}$	14	$0.92 \times 8p^1_{1/2}7d^1_{3/2}6f^3_{5/2}5g^5_{7/2}+$ $0.06 \times 8p^1_{1/2}7d^1_{3/2}6f^2_{5/2}5g^5_{7/2}6f^1_{7/2}$	14	$0.85 \times 8p^2_{1/2}6f^3_{5/2}5g^5_{7/2}+$ $0.06 \times 7d^2_{3/2}6f^3_{5/2}5g^5_{7/2}$	12	$5g^56f^37d^18p^1$
|**131**		$8p^1_{1/2}7d^1_{3/2}6f^3_{5/2}5g^6_{7/2}$	25/2	$0.82 \times 8p^2_{1/2}6f^3_{5/2}5g^6_{7/2}+$ $0.06 \times 7d^2_{3/2}6f^3_{5/2}5g^6_{7/2}+$ $0.06 \times 8p^1_{1/2}7d^2_{3/2}6f^2_{5/2}5g^6_{7/2}+$ $0.05 \times 8p^2_{1/2}6f^2_{5/2}5g^6_{7/2}6f^1_{7/2}$	21/2	$0.85 \times 8p^2_{1/2}6f^3_{5/2}5g^6_{7/2}+$ $0.05 \times 7d^2_{3/2}6f^3_{5/2}5g^6_{7/2}$	21/2	$0.86 \times 5g^66f^38p^2+$ $0.14 \times 5g^66f^27d^28p^1$
|**132**		$8p^1_{1/2}7d^1_{3/2}6f^3_{5/2}5g^7_{7/2}$	10	$0.84 \times 8p^2_{1/2}6f^3_{5/2}5g^7_{7/2}+$ $0.08 \times 8p^1_{1/2}7d^2_{3/2}6f^2_{5/2}5g^7_{7/2}+$ $0.06 \times 7d^2_{3/2}6f^3_{5/2}5g^7_{7/2}$	6	$0.87 \times 8p^2_{1/2}6f^3_{5/2}5g^7_{7/2}+$ $0.05 \times 7d^2_{3/2}6f^3_{5/2}5g^7_{7/2}$	6	$5g^76f^38p^2$
|**133**		$8p^1_{1/2}7d^1_{3/2}6f^3_{5/2}5g^8_{7/2}$	13/2	$0.83 \times 8p^2_{1/2}6f^3_{5/2}5g^8_{7/2}+$ $0.09 \times 8p^1_{1/2}7d^2_{3/2}6f^2_{5/2}5g^8_{7/2}$	9/2	$0.87 \times 8p^2_{1/2}6f^3_{5/2}5g^8_{7/2}$	9/2	$5g^86f^38p^2$
|**134**	$+5g^8_{7/2}$	$8p^1_{1/2}7d^1_{3/2}6f^4_{5/2}$	6	$0.82 \times 8p^2_{1/2}6f^4_{5/2}+$ $0.07 \times 8p^1_{1/2}7d^2_{3/2}6f^3_{5/2}+$ $0.06 \times 7d^2_{3/2}6f^4_{5/2}$	4	$0.84 \times 8p^2_{1/2}6f^4_{5/2}+$ $0.05 \times 8p^1_{1/2}7d^2_{3/2}6f^3_{5/2}+$ $0.05 \times 7d^2_{3/2}6f^4_{5/2}$	4	$5g^86f^48p^2$
|**135**		$8p^2_{1/2}7d^1_{3/2}6f^3_{5/2}5g^1_{9/2}$	13/2	$0.82 \times 8p^2_{1/2}6f^4_{5/2}5g^1_{9/2}+$ $0.08 \times 8p^1_{1/2}7d^2_{3/2}6f^3_{5/2}5g^1_{9/2}+$ $0.05 \times 7d^2_{3/2}6f^4_{5/2}5g^1_{9/2}$	5/2	$0.85 \times 8p^2_{1/2}6f^4_{5/2}5g^1_{9/2}+$ $0.06 \times 8p^1_{1/2}7d^2_{3/2}6f^3_{5/2}5g^1_{9/2}$	5/2	$5g^96f^48p^2$
136		$8p^2_{1/2}7d^1_{3/2}6f^3_{5/2}5g^2_{9/2}$	3	$0.91 \times 8p^2_{1/2}7d^1_{3/2}6f^3_{5/2}5g^2_{9/2}+$ $0.05 \times 7d^3_{3/2}6f^3_{5/2}5g^2_{9/2}$	4	$0.89 \times 8p^2_{1/2}7d^1_{3/2}6f^3_{5/2}5g^2_{9/2}$	4	$5g^{10}6f^48p^2$
|**137**|		$8p^2_{1/2}7d^1_{3/2}6f^3_{5/2}5g^3_{9/2}$	19/2	$0.80 \times 8p^2_{1/2}6f^4_{5/2}5g^3_{9/2}+$ $0.11 \times 8p^1_{1/2}7d^2_{3/2}6f^3_{5/2}5g^3_{9/2}$	13/2	$0.89 \times 8p^2_{1/2}7d^1_{3/2}6f^3_{5/2}5g^3_{9/2}$	17/2	$5g^{11}6f^48p^2$
138	$+8p^2_{1/2}$	$7d^1_{3/2}6f^3_{5/2}5g^4_{9/2}$	6	$0.91 \times 7d^1_{3/2}6f^3_{5/2}5g^4_{9/2}$	7	$0.89 \times 7d^1_{3/2}6f^3_{5/2}5g^4_{9/2}$	7	$5g^{12}6f^37d^18p^2$
139		$7d^1_{3/2}6f^3_{5/2}5g^5_{9/2}$	13/2	$0.92 \times 7d^1_{3/2}6f^3_{5/2}5g^5_{9/2}$	13/2	$0.91 \times 7d^1_{3/2}6f^3_{5/2}5g^5_{9/2}$	13/2	$5g^{13}6f^37d^18p^2$
|**140**		$7d^2_{3/2}6f^2_{5/2}5g^6_{9/2}$	6	$0.90 \times 7d^1_{3/2}6f^3_{5/2}5g^6_{9/2}+$ $0.05 \times 7d^1_{3/2}6f^2_{5/2}5g^6_{9/2}6f^1_{7/2}$	6	$0.90 \times 7d^1_{3/2}6f^3_{5/2}5g^6_{9/2}$	6	$5g^{14}6f^37d^18p^2$
141		$7d^2_{3/2}6f^2_{5/2}5g^7_{9/2}$	9/2	$0.93 \times 7d^2_{3/2}6f^2_{5/2}5g^7_{9/2}$	9/2	$0.91 \times 7d^2_{3/2}6f^2_{5/2}5g^7_{9/2}$	9/2	$5g^{15}6f^27d^28p^2$
142		$7d^2_{3/2}6f^2_{5/2}5g^8_{9/2}$	2	$0.91 \times 7d^2_{3/2}6f^2_{5/2}5g^8_{9/2}$	2	$0.89 \times 7d^2_{3/2}6f^2_{5/2}5g^8_{9/2}$	2	$5g^{16}6f^27d^28p^2$
143		$7d^2_{3/2}6f^3_{5/2}5g^8_{9/2}$	5/2	$0.93 \times 7d^2_{3/2}6f^3_{5/2}5g^8_{9/2}$	3/2	$0.92 \times 7d^2_{3/2}6f^3_{5/2}5g^8_{9/2}$	1/2	$5g^{17}6f^27d^28p^2$

TABLE VI. *(Continued.)*

Z	Closed shells	DCBQ-SRC	$J_{\rm SRC}$	DCBQ-CI1	$J_{\rm CI1}$	DCBQ-CI2	$J_{\rm CI2}$	Ref. [47]
144		$7d^2_{3/2}6f^3_{5/2}5g^9_{9/2}$	7	$0.96\times 7d^2_{3/2}6f^3_{5/2}5g^9_{9/2}$	7	$0.94\times 7d^2_{3/2}6f^3_{5/2}5g^9_{9/2}$	7	$0.95\times 5g^{17}6f^27d^38p^2+$ $0.05\times 5g^{17}6f^47d^18p^2$
145		$7d^2_{3/2}6f^3_{5/2}5g^{10}_{9/2}$	13/2	$0.96\times 7d^2_{3/2}6f^3_{5/2}5g^{10}_{9/2}$	13/2	$0.93\times 7d^2_{3/2}6f^3_{5/2}5g^{10}_{9/2}$	13/2	$5g^{18}6f^37d^28p^2$
146	$+5g^{10}_{9/2}$	$7d^2_{3/2}6f^4_{5/2}$	6	$0.95\times 7d^2_{3/2}6f^4_{5/2}$	6	$0.91\times 7d^2_{3/2}6f^4_{5/2}$	6	$6f^47d^28p^2$
147		$7d^2_{3/2}6f^5_{5/2}$	7/2	$0.89\times 7d^2_{3/2}6f^5_{5/2}+$ $0.07\times 7d^2_{3/2}6f^4_{5/2}6f^1_{7/2}$	9/2	$0.88\times 7d^2_{3/2}6f^5_{5/2}+$ $0.05\times 7d^2_{3/2}6f^4_{5/2}6f^1_{7/2}$	9/2	$6f^57d^28p^2$
148		$7d^2_{3/2}6f^6_{5/2}$	2	$0.94\times 7d^2_{3/2}6f^6_{5/2}$	2	$0.93\times 7d^2_{3/2}6f^6_{5/2}$	2	$6f^67d^28p^2$
149		$7d^3_{3/2}6f^6_{5/2}$	3/2	$0.96\times 7d^3_{3/2}6f^6_{5/2}$	3/2	$0.93\times 7d^3_{3/2}6f^6_{5/2}$	3/2	$6f^67d^38p^2$
150		$7d^3_{3/2}6f^6_{5/2}6f^1_{7/2}$	2	$0.85\times 7d^3_{3/2}6f^6_{5/2}6f^1_{7/2}+$ $0.11\times 7d^3_{3/2}6f^5_{5/2}6f^2_{7/2}$	2	$0.89\times 7d^3_{3/2}6f^6_{5/2}6f^1_{7/2}+$ $0.06\times 7d^3_{3/2}6f^5_{5/2}6f^2_{7/2}$	2	$6f^77d^38p^2$
151		$7d^3_{3/2}6f^6_{5/2}6f^2_{7/2}$	9/2	$0.89\times 7d^3_{3/2}6f^6_{5/2}6f^2_{7/2}+$ $0.09\times 7d^3_{3/2}6f^5_{5/2}6f^3_{7/2}$	9/2	$0.89\times 7d^3_{3/2}6f^6_{5/2}6f^2_{7/2}+$ $0.06\times 7d^3_{3/2}6f^5_{5/2}6f^3_{7/2}$	9/2	$6f^87d^38p^2$
152	$+6f^6_{5/2}$	$7d^2_{3/2}6f^4_{7/2}$	6	$0.95\times 7d^2_{3/2}6f^4_{7/2}$	6	$0.92\times 7d^2_{3/2}6f^4_{7/2}$	6	$6f^97d^38p^2$
153		$7d^2_{3/2}6f^5_{7/2}$	11/2	$0.96\times 7d^2_{3/2}6f^5_{7/2}$	11/2	$0.93\times 7d^2_{3/2}6f^5_{7/2}$	11/2	$6f^{10}7d^38p^2$
154		$7d^2_{3/2}6f^6_{7/2}$	6	$0.98\times 7d^2_{3/2}6f^6_{7/2}$	6	$0.95\times 7d^2_{3/2}6f^6_{7/2}$	6	$6f^{11}7d^38p^2$
|**155**		$7d^2_{3/2}6f^7_{7/2}$	7/2	$0.99\times 9s^1_{1/2}6f^8_{7/2}$	1/2	$0.94\times 9s^1_{1/2}6f^8_{7/2}$	1/2	$6f^{12}7d^38p^2$
156		$7d^2_{3/2}6f^8_{7/2}$	2	$0.97\times 7d^2_{3/2}6f^8_{7/2}$	2	$0.97\times 7d^2_{3/2}6f^8_{7/2}$	2	$6f^{13}7d^38p^2$
157	$+6f^8_{7/2}$	$7d^3_{3/2}$	3/2	$0.96\times 7d^3_{3/2}$	3/2	$0.96\times 7d^3_{3/2}$	3/2	$6f^{14}7d^38p^2$
158		$7d^4_{3/2}$	0	$0.98\times 7d^4_{3/2}$	0	$0.96\times 7d^4_{3/2}$	0	$6f^{14}7d^48p^2$
159	$+7d^4_{3/2}$	$9s^1_{1/2}$	1/2	$0.98\times 9s^1_{1/2}$	1/2	$0.96\times 9s^1_{1/2}$	1/2	$6f^{14}7d^48p^29s^1$
160		$7d^1_{5/2}9s^1_{1/2}$	3	$0.96\times 7d^1_{5/2}9s^1_{1/2}$	3	$0.95\times 7d^1_{5/2}9s^1_{1/2}$	3	$6f^{14}7d^58p^29s^1$
161		$7d^2_{5/2}9s^1_{1/2}$	9/2	$0.97\times 7d^2_{5/2}9s^1_{1/2}$	9/2	$0.92\times 7d^2_{5/2}9s^1_{1/2}$	9/2	$6f^{14}7d^68p^29s^1$
162		$7d^3_{5/2}9s^1_{1/2}$	5	$0.98\times 7d^3_{5/2}9s^1_{1/2}$	5	$0.96\times 7d^3_{5/2}9s^1_{1/2}$	5	$6f^{14}7d^78p^29s^1$
163		$7d^5_{5/2}$	5/2	$0.96\times 7d^5_{5/2}$	5/2	$0.95\times 7d^5_{5/2}$	5/2	$6f^{14}7d^88p^29s^1$
164		$7d^6_{5/2}$	0	$0.98\times 7d^6_{5/2}$	0	$0.96\times 7d^6_{5/2}$	0	$6f^{14}7d^{10}8p^2$
165	$+7d^6_{5/2}$	$9s^1_{1/2}$	1/2	$0.98\times 9s^1_{1/2}$	1/2	$0.96\times 9s^1_{1/2}$	1/2	
166		$9s^2_{1/2}$	0	$0.84\times 9s^2_{1/2}+0.10\times 8p^2_{3/2}$	0	$0.90\times 9s^2_{1/2}$	0	
|**167**		$9s^1_{1/2}8p^1_{3/2}9p^1_{1/2}$	3/2	$0.88\times 9s^2_{1/2}8p^1_{3/2}+0.06\times 8p^3_{3/2}$	3/2	$0.91\times 9s^2_{1/2}8p^1_{3/2}$	3/2	
|168|		$9s^2_{1/2}8p^1_{3/2}9p^1_{1/2}$	1	$0.55\times 9s^1_{1/2}8p^2_{3/2}9p^1_{1/2}+$ $0.24\times 9s^1_{1/2}8p^1_{3/2}9p^2_{1/2}+$ $0.20\times 9s^1_{1/2}8p^3_{3/2}$	2	$0.94\times 9s^2_{1/2}8p^1_{3/2}9p^1_{1/2}$	1	
169		$9s^2_{1/2}8p^2_{3/2}9p^1_{1/2}$	3/2	$0.76\times 9s^2_{1/2}8p^2_{3/2}9p^1_{1/2}+$ $0.16\times 9s^2_{1/2}8p^1_{3/2}9p^2_{1/2}+$ $0.06\times 9s^2_{1/2}8p^3_{3/2}$	3/2	$0.83\times 9s^2_{1/2}8p^2_{3/2}9p^1_{1/2}+$ $0.07\times 9s^2_{1/2}8p^1_{3/2}9p^2_{1/2}$	3/2	
170		$9s^2_{1/2}8p^2_{3/2}9p^2_{1/2}$	2	$0.96\times 9s^2_{1/2}8p^2_{3/2}9p^2_{1/2}$	2	$0.93\times 9s^2_{1/2}8p^2_{3/2}9p^2_{1/2}$	2	

the previous multiconfiguration Dirac-Fock calculations [47]. The nonrelativistic notations of Ref. [47] are retained.

A comparison of Tables V and VI shows that the configurations of the ground levels obtained within the SRC approach differ from the RAV ground-state configurations in almost half of the cases (for convenience, the corresponding values of Z are in bold). This result indicates the complex level structure of the SHEs, which is discussed in detail for $Z = 125$ in Sec. III.

The subsequent discussion consists of two parts. At first, we identify general trends for the results of the many-configuration calculations and compare them with the single-configuration ones. We note that the DCBQ-CI1 and DCBQ-CI2 results are, in general, not much different. Therefore, in this part we often drop the indices 1 or 2 and use the generalized designation "DCBQ-CI" for the many-configuration calculations. In the second part, we compare the results obtained by the configuration-interaction method CI1 and CI2 with each other.

Exactly as the DCBQ-RAV scheme predicts, our many-configuration DCBQ-CI results detect the first appearance of the $5g$ electron in the ground state for the SHE with $Z = 125$. However, in contrast to the DCBQ-RAV results, the DCBQ-CI schemes predict that the $5g$ shell becomes closed for $Z = 145$ instead of $Z = 144$. In the range $Z = 125$–132, the many-configuration calculations reveal that the dominant configurations of the obtained ground-state levels in all eight cases differ from the ones obtained within the DCBQ-RAV approach. Moreover, a configuration mixing in the ground states takes place for some SHEs in the range $Z = 125$–145 as the $5g$ shells are gradually occupied. In most of the considered cases, the weights of the dominant configurations lie in range 0.80 – 0.90. The configurations with different occupation numbers for the $8p_{1/2}$, $7d_{3/2}$, $6f_{5/2}$, and $5g_{7/2,9/2}$ shells are admixed. The DCBQ-CI schemes show that starting from $Z = 130$ the dominant configuration of the ground-state level has the $8p_{1/2}$ shell fully occupied. However, the configurations with the partially occupied $8p_{1/2}$ shell contribute

(with weights about 0.05 or higher) to these levels up to approximately $Z \approx 135$–137.

A mixture of the configurations with the partially occupied $7d_{3/2}$ and $6f_{5/2}$ shells occurs also in the range $Z = 147$–151. The situation with the ground states becomes more clear starting from the SHE with $Z = 152$, when the $6f_{5/2}$ shell turns out to be fully occupied. Up to $Z = 165$, the weights of the dominant configurations are larger than 0.90, and in most of the cases the dominant configurations of the ground-state levels coincide with the ground-state configurations obtained within the DCBQ-RAV approach. In particular, the fact that the SHE with $Z = 164$ possesses the ground-state configuration with all the relativistic shells closed is confirmed by the more elaborated methods. The SHEs with $Z = 168$ and $Z = 169$ demonstrate within the DCBQ-CI1 scheme poorly resolved dominant configurations of the ground-state levels. For instance, the DCBQ-CI1 weight of the dominant configuration for $Z = 168$ is only 0.55, which was not the case even for the SHEs with the open $5g_{7/2}$ and $5g_{9/2}$ shells. However, increasing the number of active orbitals remedies the situation, and for $Z = 168$ the DCBQ-CI2 scheme yields the dominant-configuration weight equal to 0.92. This is due to the fact that the levels interchange, see the corresponding discussion in Sec. III.

The overall trends obtained in our many-configuration calculations are the following. First, the configurations which have the lowest levels within the DCBQ-SRC approach are the dominant ones contributing to the ground-state levels within the DCBQ-CI approach in about 80% of the considered cases. Second, the ground-state levels obtained without the electronic correlations using the DCBQ-SRC scheme in about 75% of the cases coincide with the ones obtained by means of the DCBQ-CI approach. The deviations are mainly concentrated in the range $Z = 131$–138, where the $5g_{7/2}$ and $5g_{9/2}$ shells are partially occupied and strong interaction between several configurations takes place. The simultaneous change of the dominant configuration and the ground-state level when passing from the DCBQ-SRC to the DCBQ-CI method occurs for, e.g., $Z = 131$. In this case the first scheme yields $J_{\rm SRC} = 25/2$ of the configuration $K_{\rm SRC} = 8p^1_{1/2}7d^1_{3/2}6f^3_{5/2}5g^6_{7/2}$, whereas the second scheme predicts the lowest level to be $J_{\rm CI} = 21/2$, with the dominant configuration being $K_{\rm CI} = 8p^2_{1/2}6f^3_{5/2}5g^6_{7/2}$ with a weight of about 0.82–0.85.

Now we proceed to contrast the two DCBQ-CI schemes results. Compared to the DCBQ-CI1 data, the more accurate treatment of the electron-electron correlations by means of the DCBQ-CI2 approach results in the changes of the ground-state level in four of 51 cases. In three of these four cases, the configuration which gives the maximum contribution to the ground-state level changes as well. These SHEs, which need particular attention, are the ones with $Z = 130$, 137, 143, and 168. For instance, for $Z = 130$, the level $J = 14$ of the dominant configuration $K = 8p^1_{1/2}7d^1_{3/2}6f^3_{5/2}5g^5_{7/2}$ is predicted to be the ground-state one in both DCBQ-SRC and DCBQ-CI1 schemes: $K_{\rm SRC} = K_{\rm CI1} = K$. However, the electronic correlations evaluated by means of the DCBQ-CI2 scheme change the ground-state level, and it becomes $J = 12$, with the dominant configuration being $K_{\rm CI2} = 8p^2_{1/2}6f^3_{5/2}5g^5_{7/2} \neq K$.

We compare our DCBQ-CI2 results with the only available systematic many-configuration calculations of Ref. [47], where the Breit interaction was taken into account as well. Since the quantum numbers J which characterize the ground-state levels are not presented in that paper, we are able to compare only the configurations. We found a disagreement in the configurations contributing to the ground states for the SHEs with $Z = 123$–128, $Z = 130$, $Z = 136$–137, $Z = 143$–144, $Z = 152$–156, and $Z = 163$. It is difficult to reveal a possible reason for the discrepancy due to the lack of computational details given in Ref. [47].

The changes of the ground-state levels in transition from the DCBQ-CI1 to the DCBQ-CI2 calculations and the deviations from the previous results raise the following question: can hypothetical larger CI calculations change the obtained ground states as the DCBQ-CI2 scheme changes the ground states in comparison with the DCBQ-CI1 one? A comprehensive answer can be given only within the scope of the corresponding large-scale CI calculations. However, to get an idea of the cases for which the correlation effects may change the dominant configuration of the ground-state level, we investigate the behavior of the energy difference between the ground-state level and the closest level belonging to a different dominant configuration for both our DCBQ-CI calculations. This study allows us to determine whether the ground-state level is in some sense isolated from levels of other configurations and whether the electronic correlations break down this isolation. The absolute values of the corresponding differences are presented in Table VII. Before discussing Table VII, we emphasize that it shows the numerical results for two specific calculations, whose reliability we want to determine. The values presented in Table VII serve to provide clues to some general trends, and they do not purport to give the exact results for the distances between the corresponding energy levels. The SHE with $Z = 120$ is omitted in Table VII, since it possesses the ground-state configuration $K^* = [\mathrm{Og}]8s^2_{1/2}$ that causes no doubt.

As it is seen from Table VII, some SHEs have a clear separation of the ground-state level from levels of other configurations, which almost does not depend on the correlation-treatment scheme. For instance, for $Z = 121$, the separations of the levels in the DCBQ-CI1 and DCBQ-CI2 schemes constitute 0.0399 a.u. and 0.0378 a.u., respectively. In other cases, the ground-state level becomes more isolated from the levels of other configurations as the correlation treatment is improved. So, for $Z = 155$, the separation increases from 0.0108 a.u. in the DCBQ-CI1 scheme to 0.0257 a.u. in the DCBQ-CI2 one. In spite of this, it is difficult to formulate for all the systems under consideration a reliable criteria to determine whether the dominant configuration contributing to the ground-state level does change with increase of the configuration-space. From this point of view, the most suspicious SHEs are the ones which have a small (less than a few thousandths of a.u.) separation between the considered levels within the DCBQ-CI2 scheme. In addition, we also include in this category the cases where the separation between the levels significantly decreases in the DCBQ-CI2 scheme compared to the DCBQ-CI1 results as well as the cases where the dominant configurations are different in the two calculations. Analyzing the data in Table VII, we consider the SHEs

TABLE VII. The absolute values of the energy difference between the ground-state level of the dominant configuration K^* and the closest excited level belonging to the dominant configuration, which is different from K^* for the SHEs in the range $121 \leqslant Z \leqslant 170$ (a.u.). The results are presented for the DCBQ-CI1 and DCBQ-CI2 schemes.

Z	CI1	CI2	Z	CI1	CI2	Z	CI1	CI2	Z	CI1	CI2	Z	CI1	CI2
121	0.0399	0.0378	131	0.0047	0.0069	141	0.0195	0.0106	151	0.0176	0.0114	161	0.0103	0.0059
122	0.0127	0.0107	132	0.0083	0.0118	142	0.0143	0.0046	152	0.0059	0.0122	162	0.0094	0.0016
123	0.0299	0.0351	133	0.0254	0.0204	143	0.0015	0.0116	153	0.0062	0.0129	163	0.0111	0.0176
124	0.0050	0.0046	134	0.0313	0.0270	144	0.0013	0.0129	154	0.0107	0.0008	164	0.0492	0.0542
125	0.0062	0.0057	135	0.0165	0.0125	145	0.0539	0.0376	155	0.0108	0.0257	165	0.0424	0.0443
126	0.0106	0.0126	136	0.0062	0.0095	146	0.0352	0.0273	156	0.0136	0.0110	166	0.0153	0.0305
127	0.0070	0.0089	137	0.0011	0.0043	147	0.0398	0.0349	157	0.0208	0.0212	167	0.0022	0.0096
128	0.0116	0.0123	138	0.0248	0.0303	148	0.0715	0.0760	158	0.0529	0.0555	168	0.0244	0.0091
129	0.0071	0.0034	139	0.0370	0.0322	149	0.0583	0.0568	159	0.0568	0.0581	169	0.0066	0.0087
130	0.0022	0.0009	140	0.0237	0.0088	150	0.0295	0.0300	160	0.0308	0.0285	170	0.0287	0.0324

with $Z = 129$, 130, 137, 140, 142, 154, 161, 162, and 168 as those that can possibly have a different dominant configuration of the ground-state level than the one obtained within the DCBQ-CI2 scheme. These elements have to be studied within the more elaborated electron-correlation calculations.

V. CONCLUSION

In the scope of the present paper, we have performed the extensive relativistic study of the ground states of the superheavy elements in the range $120 \leqslant Z \leqslant 170$. The Breit interaction is rigorously taken into account in the calculations, and the QED effects are considered within the model-QED-operator approach [51–53]. The ground-state configurations are first determined by means of the Dirac-Fock method in the relativistic-configuration-average approximation. It is deduced that the QED effects cannot change the ground-state configuration, in contrast to the Breit interaction.

To resolve the level structure of the configurations, the ground-state levels are found using the configuration-interaction method in the basis of the Dirac-Fock-Sturm orbitals. We study the general trends in the order of occupation of orbitals in the SHE. We obtain that in spite of the complex electronic structure of the considered SHEs, the ground-state levels have distinct dominant configurations with the weights exceeding 0.85. Finally, we demonstrate that the electron-correlation effects can change the dominant configuration of the ground-state level. For some SHEs, large-scale calculations are needed in order to more reliably determine the ground states and the structure of low-lying energy levels. Nevertheless, the ground-state configurations of the SHEs obtained in the present work within the many-configuration approach can be used as a solid basis for accurate calculations of various atomic properties of these elements as well as to examine the role of the electron-electron correlations, QED, and relativistic effects on the periodic law.

ACKNOWLEDGMENTS

We thank Yu. Ts. Oganessian for stimulating discussions. Valuable conversations with E. Eliav, V. Pershina, and A. V. Titov are also gratefully acknowledged. The work was supported by the Ministry of Science and Higher Education of the Russian Federation within Grant No. 075-10-2020-117.

[1] P. Pyykko and J. P. Desclaux, Acc. Chem. Res. **12**, 276 (1979).
[2] P. Pyykko, Chem. Rev. **88**, 563 (1988).
[3] P. Pyykkö, Chem. Rev. **112**, 371 (2012).
[4] Y. T. Oganessian and V. K. Utyonkov, Rep. Prog. Phys. **78**, 036301 (2015).
[5] Y. T. Oganessian, A. Sobiczewski, and G. M. Ter-Akopian, Phys. Scr. **92**, 023003 (2017).
[6] V. Pershina, Nucl. Phys. A **944**, 578 (2015).
[7] V. Pershina, Radiochim. Acta **107**, 833 (2019).
[8] S. A. Giuliani, Z. Matheson, W. Nazarewicz, E. Olsen, P.-G. Reinhard, J. Sadhukhan, B. Schuetrumpf, N. Schunck, and P. Schwerdtfeger, Rev. Mod. Phys. **91**, 011001 (2019).
[9] T. K. Sato, M. Asai, A. Borschevsky, T. Stora, N. Sato, Y. Kaneya, K. Tsukada, C. E. Düllmann, K. Eberhardt, E. Eliav, S. Ichikawa, U. Kaldor, J. V. Kratz, S. Miyashita, Y. Nagame, K. Ooe, A. Osa, D. Renisch, J. Runke, M. Schädel *et al.*, Nature (London) **520**, 209 (2015).
[10] E. Eliav, U. Kaldor, Y. Ishikawa, and P. Pyykkö, Phys. Rev. Lett. **77**, 5350 (1996).
[11] I. Goidenko, L. Labzowsky, E. Eliav, U. Kaldor, and P. Pyykkö, Phys. Rev. A **67**, 020102(R) (2003).
[12] B. G. C. Lackenby, V. A. Dzuba, and V. V. Flambaum, Phys. Rev. A **98**, 042512 (2018).
[13] Y. Guo, L. F. Pašteka, E. Eliav, and A. Borschevsky, Adv. Quantum Chem. **83**, 107 (2021).
[14] M. Y. Kaygorodov, L. V. Skripnikov, I. I. Tupitsyn, E. Eliav, Y. S. Kozhedub, A. V. Malyshev, A. V. Oleynichenko, V. M. Shabaev, A. V. Titov, and A. V. Zaitsevskii, Phys. Rev. A **104**, 012819 (2021).
[15] P. Pyykkö, Phys. Chem. Chem. Phys. **13**, 161 (2011).
[16] O. R. Smits, P. Indelicato, W. Nazarewicz, M. Piibeleht, and P. Schwerdtfeger, arXiv:2301.02553.
[17] I. Pomeranchuk and J. Smorodinsky, J. Phys. USSR **9**, 97 (1945).
[18] V. Voronkov and N. Kolesnikov, Zh. Eksp. Teor. Fiz. **39**, 189 (1961), [Sov. Phys. JETP **12**, 136 (1961)].

[19] S. S. Gershtein and Y. B. Zel'dovich, Zh. Eksp. Teor. Fiz. **57**, 654 (1969); Sov. Phys. JETP **30**, 358 (1970); Lett. Nuovo Cimento **1**, 835 (1969).

[20] W. Pieper and W. Greiner, Z. Phys. **218**, 327 (1969).

[21] Y. B. Zel'dovich and V. S. Popov, Usp. Fiz. Nauk **105**, 403 (1971) [Sov. Phys. Usp. **14**, 673 (1972)].

[22] W. Greiner, B. Müller, and J. Rafelski, *Quantum Electrodynamics of Strong Fields*, 1st ed., (Springer Berlin, Heidelberg, 1985).

[23] V. S. Popov, Yad. Fiz. **64**, 421 (2001) [Phys. At. Nucl. **64**, 367 (2001)].

[24] S. I. Godunov, B. Machet, and M. I. Vysotsky, Eur. Phys. J. C **77**, 782 (2017).

[25] J. Rafelski, J. Kirsch, B. Müller, J. Reinhardt, and W. Greiner, *Probing QED Vacuum with Heavy Ions* (Springer, Cham, 2017), pp. 211–251.

[26] R. V. Popov, V. M. Shabaev, D. A. Telnov, I. I. Tupitsyn, I. A. Maltsev, Y. S. Kozhedub, A. I. Bondarev, N. V. Kozin, X. Ma, G. Plunien, T. Stöhlker, D. A. Tumakov, and V. A. Zaytsev, Phys. Rev. D **102**, 076005 (2020).

[27] D. N. Voskresensky, Universe **7**, 104 (2021).

[28] A. Krasnov and K. Sveshnikov, Mod. Phys. Lett. A **37**, 2250136 (2022).

[29] J. B. Mann and J. T. Waber, J. Chem. Phys. **53**, 2397 (1970).

[30] C. Lu, T. Carlson, F. Malik, T. Tucker, and C. Nestor, At. Data Nucl. Data Tables **3**, 1 (1971).

[31] B. Fricke, W. Greiner, and J. T. Waber, Theor. Chim. Acta **21**, 235 (1971).

[32] B. Fricke and J. T. Waber, J. Chem. Phys. **57**, 371 (1972).

[33] J. Desclaux, At. Data Nucl. Data Tables **12**, 311 (1973).

[34] B. Fricke and G. Soff, At. Data Nucl. Data Tables **19**, 83 (1977).

[35] K. Umemoto and S. Saito, J. Phys. Soc. Jpn. **65**, 3175 (1996).

[36] Z. Zhou, J. Kas, J. Rehr, and W. Ermler, At. Data Nucl. Data Tables **114**, 262 (2017).

[37] E. Eliav, S. Shmulyian, U. Kaldor, and Y. Ishikawa, J. Chem. Phys. **109**, 3954 (1998).

[38] E. Eliav, A. Landau, Y. Ishikawa, and U. Kaldor, J. Phys. B: At., Mol. Opt. Phys. **35**, 1693 (2002).

[39] I. S. Lim, P. Schwerdtfeger, B. Metz, and H. Stoll, J. Chem. Phys. **122**, 104103 (2005).

[40] P. Indelicato, J. P. Santos, S. Boucard, and J.-P. Desclaux, Eur. Phys. J. D **45**, 155 (2007).

[41] P. Indelicato, J. Bieroń, and P. Jönsson, Theor. Chem. Acc. **129**, 495 (2011).

[42] L. V. Skripnikov, N. S. Mosyagin, and A. V. Titov, Chem. Phys. Lett. **555**, 79 (2013).

[43] A. Borschevsky, V. Pershina, E. Eliav, and U. Kaldor, J. Chem. Phys. **138**, 124302 (2013).

[44] J. S. M. Ginges and J. C. Berengut, Phys. Rev. A **93**, 052509 (2016); J. Phys. B: At., Mol. Opt. Phys. **49**, 095001 (2016).

[45] A. V. Zaitsevskii, Y. A. Demidov, N. S. Mosyagin, L. V. Skripnikov, and A. V. Titov, Rad. Applic. **1**, 132 (2016).

[46] I. I. Tupitsyn, A. V. Malyshev, D. A. Glazov, M. Y. Kaygorodov, Y. S. Kozhedub, I. M. Savelyev, and V. M. Shabaev, Opt. Spektrosk. **129**, 841 (2021) [Opt. Spectrosc. **129**, 1038 (2021)].

[47] V. I. Nefedov, M. B. Trzhaskovskaya, and V. G. Yarzhemskii, Dokl. Phys. Chem. **408**, 149 (2006).

[48] I. I. Tupitsyn, V. M. Shabaev, J. R. Crespo López-Urrutia, I. Draganić, R. Soria Orts, and J. Ullrich, Phys. Rev. A **68**, 022511 (2003).

[49] I. I. Tupitsyn, A. V. Volotka, D. A. Glazov, V. M. Shabaev, G. Plunien, J. R. Crespo López-Urrutia, A. Lapierre, and J. Ullrich, Phys. Rev. A **72**, 062503 (2005).

[50] I. I. Tupitsyn, N. A. Zubova, V. M. Shabaev, G. Plunien, and T. Stöhlker, Phys. Rev. A **98**, 022517 (2018).

[51] V. M. Shabaev, I. I. Tupitsyn, and V. A. Yerokhin, Phys. Rev. A **88**, 012513 (2013).

[52] V. M. Shabaev, I. I. Tupitsyn, and V. A. Yerokhin, Comput. Phys. Commun. **189**, 175 (2015); **223**, 69 (2018).

[53] A. V. Malyshev, D. A. Glazov, V. M. Shabaev, I. I. Tupitsyn, V. A. Yerokhin, and V. A. Zaytsev, Phys. Rev. A **106**, 012806 (2022).

[54] I. Lindgren and A. Rosen, Case Stud. At. Phys. IV **4**, 93 (1975).

[55] I. P. Grant, Proc. R. Soc. London A **262**, 555 (1961).

[56] I. Grant, Adv. Phys. **19**, 747 (1970).

[57] P. Indelicato and J. P. Desclaux, Phys. Rev. A **42**, 5139 (1990).

[58] P. Pyykkö and L.-B. Zhao, J. Phys. B: At. Mol. Opt. Phys. **36**, 1469 (2003).

[59] I. Draganić, J. R. Crespo López-Urrutia, R. DuBois, S. Fritzsche, V. M. Shabaev, R. S. Orts, I. I. Tupitsyn, Y. Zou, and J. Ullrich, Phys. Rev. Lett. **91**, 183001 (2003).

[60] V. V. Flambaum and J. S. M. Ginges, Phys. Rev. A **72**, 052115 (2005).

[61] C. Thierfelder and P. Schwerdtfeger, Phys. Rev. A **82**, 062503 (2010).

[62] I. I. Tupitsyn and E. V. Berseneva, Opt. Spektrosk. **114**, 743 (2013); Opt. Spectrosc. **114**, 682 (2013).

[63] L. V. Skripnikov, J. Chem. Phys. **154**, 201101 (2021).

[64] L. V. Skripnikov, D. V. Chubukov, and V. M. Shakhova, J. Chem. Phys. **155**, 144103 (2021).

[65] A. Sunaga and T. Saue, Mol. Phys. **119**, e1974592 (2021).

[66] A. Sunaga, M. Salman, and T. Saue, J. Chem. Phys. **157**, 164101 (2022).

[67] A. Zaitsevskii, N. S. Mosyagin, A. V. Oleynichenko, and E. Eliav, Int. J. Quantum Chem., e27077 (2022).

[68] A. V. Oleynichenko, A. Zaitsevskii, N. S. Mosyagin, A. N. Petrov, E. Eliav, and A. V. Titov, Symmetry **15**, 197 (2023).